Synthesis, structures, and properties of spiro[6-azaperimidine-2,4′-cyclohexa-2′,5′-dien]-1′-one derivatives

V. N. Komissarov,[a] E. N. Gruzdeva,[a] V. A. Kharlanov,[a] L. P. Olekhnovich,[a] G. S. Borodkin,[a] V. N. Khrustalev,[b] S. V. Lindeman,[b] Yu. T. Struchkov,[b†] V. A. Kogan,[a] and V. I. Minkin[a]*

[a]*Institute of Physical and Organic Chemistry, Rostov State University, 194/2 prosp. Stachki, 344771 Rostov-on-Don, Russian Federation. Fax: 007 (863 2) 28 5667*

[b]*A. N. Nesmeyanov Institute of Organoelement Compounds, Russian Academy of Sciences, 28 ul. Vavilova, 117813 Moscow, Russian Federation. Fax: 007 (095) 135 5085*

The reaction of 5-amino-4-chloroquinolines with 4-amino-2,6-di-*tert*-butylphenol yielded derivatives of spiro[6-azaperimidine-2,4′-cyclohexa-2′,5′-dien]-1′-one, which exhibit photo- and thermochromic properties in solutions. The structure of 2′,6′-di-*tert*-butyl-5,7,9-trimethylspiro[6-aza-2,3-dihydroperimidine-2,4′-cyclohexa-2′,5′-dien]-1′-one was established by X-ray diffraction study. The ring-chain isomerization of 2′,6′-di-*tert*-butyl-5,7-dimethyl- and 2′,6′-di-*tert*-butyl-5,7,8-trimethylspiro[6-aza-2,3-dihydroperimidine-2,4′-cyclohexa-2′,5′-dien]-1′-ones was studied by dynamic NMR spectroscopy.

Key words: 2′,6′-di-*tert*-butyl-5,7-dimethylspiro[6-aza-2,3-dihydroperimidine-2,4′-cyclohexa-2′,5′-dien]-1′-one, 2′,6′-di-*tert*-butyl-5,7,8-trimethylspiro[6-aza-2,3-dihydroperimidine-2,4′-cyclohexa-2′,5′-dien]-1′-one, photochromism and thermochromism, ring-chain isomerization, X-ray structural analysis, dynamic NMR spectroscopy.

Previously,[1] we have prepared *N*-aryl derivatives of quinazolinespiro(cyclohexa-2,5-dienone), which exhibit photo- and thermochromic properties in solutions. In this work, we synthesized spiranes of this series, which do not contain aryl substituents at the nitrogen atom, and studied their properties.

The reaction of aminochloroquinolines **1a—c** with 4-amino-2,6-di-*tert*-butylphenol (**2**) proceeded readily

Scheme 1

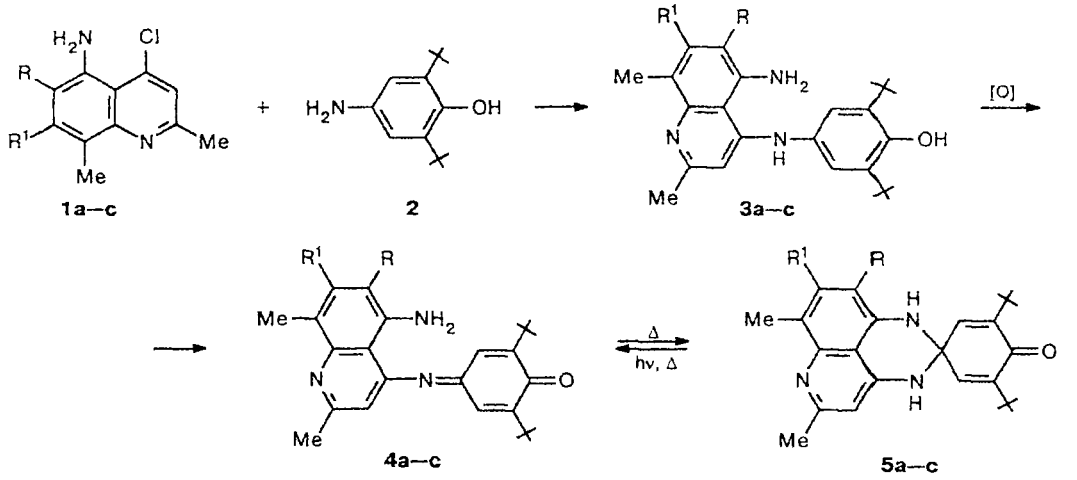

R = R¹ = H (**a**); R = H, R¹ = Me (**b**); R = Me, R¹ = H (**c**)

†Deceased.

Translated from *Izvestiya Akademii Nauk. Seriya Khimicheskaya*, No. 11, pp. 2028—2034, November, 1997.

1066-5285/97/4611-1924 $18.00

to form aminophenol hydrochlorides **3a—c**. Their bases were oxidized by atmospheric oxygen in a chloroform solution to quinone imines **4a—c** (Scheme 1).

Apparently, this oxidation proceeds analogously to oxidation of sterically hindered 4,4-dihydroxydiphenylamine to indophenol.[2]

Spirane **5c** was studied by X-ray diffraction study. The principal geometric parameters are given in Tables 1 and 2. The structure of the molecule is shown in Fig. 1. The cyclohexadiene fragment adopts a boat conformation (the C(1′) and C(4′) atoms deviate from the plane through the remaining atoms (planar to within 0.003 Å) by 0.125 and 0.101 Å, respectively). The hydrogenated pyrimidine ring adopts a sofa conformation (the C(4′) atom deviates from the plane (to within 0.003 Å) through the remaining atoms by −0.577 Å). The angle between the planes of the cyclohexadiene and pyrimidine fragments is −85.8°. The N(2) and N(3) atoms have a pyramidal configuration (the sums of the bond angles at the N(2) and N(3) atoms are 344(6)° and 349(6)°, respectively). In the crystal, the molecules are packed in stacks along the *y* axis. In stacks, the molecules are linked in helices about the axis 2_1 through the

Table 1. Bond lengths (*d*) in the structure of 5c

Bond	*d*/Å	Bond	*d*/Å
C(1′)—O(1′)	1.223(4)	N(2)—C(5)	1.405(4)
C(1′)—C(2′)	1.499(4)	N(3)—C(4)	1.378(4)
C(1′)—C(6′)	1.498(4)	C(2)—C(3)	1.402(4)
C(2′)—C(3′)	1.336(4)	C(2)—C(11)	1.497(5)
C(2′)—C(7′)	1.539(5)	C(3)—C(4)	1.379(4)
C(3′)—C(4′)	1.497(4)	C(4)—C(10)	1.413(4)
C(4′)—C(5′)	1.500(4)	C(5)—C(6)	1.379(4)
C(4′)—N(2)	1.467(4)	C(5)—C(10)	1.418(5)
C(4′)—N(2)	1.471(4)	C(6)—C(7)	1.417(5)
C(5′)—C(6′)	1.330(4)	C(6)—C(12)	1.505(5)
C(6′)—C(11′)	1.538(4)	C(7)—C(8)	1.373(5)
C(7′)—C(8′)	1.531(4)	C(8)—C(9)	1.419(4)
C(7′)—C(9′)	1.536(5)	C(8)—C(13)	1.500(5)
C(7′)—C(10′)	1.526(4)	C(9)—C(10)	1.414(4)
C(11′)—C(12′)	1.528(5)	O(1s)—C(2s)	1.260(5)
C(11′)—C(13′)	1.535(4)	O(2s)—C(2s)	1.277(5)
C(11′)—C(14′)	1.534(5)	O(2s)—C(3s)	1.501(5)
N(1)—C(2)	1.322(4)	C(1s)—C(2s)	1.449(6)
N(1)—C(9)	1.380(4)	C(3s)—C(4s)	1.437(6)

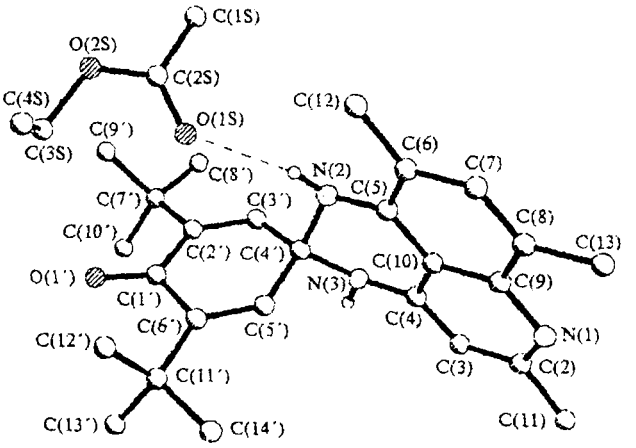

Fig. 1. Overall view of molecule **5c** (the hydrogen atoms of the amine groups, which are involved in hydrogen bonding, are shown; other hydrogen atoms are omitted for clarity); the hydrogen bond with the solvate ethyl acetate molecule is indicated by a dashed line.

Table 2. Bond angles (ω) in the structure of 5c

Angle	ω/deg	Angle	ω/deg	Angle	ω/deg
O(1′)—C(1′)—C(2′)	120.5(3)	C(2′)—C(7′)—C(10′)	110.0(3)	C(7)—C(6)—C(12)	120.8(3)
O(1′)—C(1′)—C(6′)	120.7(3)	C(8′)—C(7′)—C(10′)	108.1(3)	C(6)—C(7)—C(8)	124.1(3)
C(2′)—C(1′)—C(6′)	118.8(2)	C(9′)—C(7′)—C(10′)	109.3(3)	C(7)—C(8)—C(9)	118.1(3)
C(1′)—C(2′)—C(3′)	118.5(3)	C(6′)—C(11′)—C(12′)	109.9(3)	C(7)—C(8)—C(13)	121.2(3)
C(1′)—C(2′)—C(7′)	118.7(2)	C(6′)—C(11′)—C(13′)	110.7(3)	C(9)—C(8)—C(13)	120.7(3)
C(3′)—C(2′)—C(7′)	122.8(3)	C(12′)—C(11′)—C(13′)	109.8(3)	N(1)—C(9)—C(8)	119.1(3)
C(2′)—C(3′)—C(4′)	124.8(3)	C(4′)—N(2′)—C(5′)	117.8(2)	N(1)—C(9)—C(10)	122.0(3)
C(3′)—C(4′)—C(5′)	112.9(2)	C(4′)—N(3)—C(4)	117.9(2)	C(8)—C(9)—C(10)	118.8(3)
C(3′)—C(4′)—N(2)	107.8(2)	N(1)—C(2)—C(3)	124.4(3)	C(4)—C(10)—C(5)	120.0(3)
C(5′)—C(4′)—N(2)	110.8(2)	N(1)—C(2)—C(11)	116.7(3)	C(4)—C(10)—C(9)	118.8(3)
C(3′)—C(4′)—N(3)	108.1(2)	C(3)—C(2)—C(11)	118.9(3)	C(5)—C(10)—C(9)	121.2(3)
C(5′)—C(4′)—N(3)	109.8(2)	C(2)—C(3)—C(4)	119.5(3)	C(2s)—O(2s)—C(3s)	118.6(3)
N(2)—C(4′)—N(3)	107.3(2)	N(3)—C(4)—C(3)	123.0(3)	C(6′)—C(11′)—C(14′)	110.8(2)
C(4′)—C(5′)—C(6′)	125.3(3)	N(3)—C(4)—C(10)	118.9(3)	C(12′)—C(11′)—C(14′)	108.9(3)
C(1′)—C(6′)—C(5′)	118.3(3)	C(3)—C(4)—C(10)	118.0(3)	C(13′)—C(11′)—C(14′)	106.6(3)
C(1′)—C(6′)—C(11′)	118.6(2)	N(2)—C(5)—C(6)	122.5(3)	C(2)—N(1)—C(9)	117.1(3)
C(5′)—C(6′)—C(11′)	123.1(3)	N(2)—C(5)—C(10)	117.5(3)	O(1s)—C(2s)—O(2s)	121.4(3)
C(2′)—C(7′)—C(8′)	111.2(2)	C(6)—C(5)—C(10)	119.9(3)	O(1s)—C(2s)—C(1s)	124.4(3)
C(2′)—C(7′)—C(9′)	110.0(3)	C(5)—C(6)—C(7)	117.8(3)	O(2s)—C(2s)—C(1s)	114.1(4)
C(8′)—C(7′)—C(9′)	108.1(3)	C(5)—C(6)—C(12)	121.4(3)	O(2s)—C(3s)—C(4s)	109.6(3)

weak N(1) (1 + x, 0.5 + y, 1.5 − z)...H(3n)—N(3) hydrogen bonds (N(1)...N(3) is 3.232(5) Å, N(1)...H(3n) is 2.42(5) Å, and the N...H—N angle is 163(3)°). The solvate ethyl acetate molecule is linked to molecule **5c** *via* the weak O(1s) (1 −x, 1 − y, 2 − z)...H(2n)—N(2) hydrogen bond (O(1s)...N(2) is 3.020(5) Å, O(1s)...H(2n) is 2.20(6) Å, and the O...H—N angle is 160(4)°).

In the case of quinone imines **4a,b**, reversible ring-chain isomerization occurs (Scheme 2). Spirocyclic isomers **5a,b** of these compounds are readily identified in the ^{1}H NMR spectra from the characteristic signals of the *tert*-butyl groups. Thus, the ^{1}H NMR spectra of compounds **4a,b** have two nine-proton singlets (at δ 1.37 and 1.48 for **4a** and at δ 1.36 and 1.49 for **4b**). These singlets are assigned to two *tert*-butyl groups, which are in different chemical environments with respect to the C=N bond. On the contrary, in the case of their spirane tautomers **5a,b**, the *tert*-butyl groups are isochronous (18-proton singlets at δ 1.34) because there is an effective symmetry plane, which involves three rings.

Scheme 2

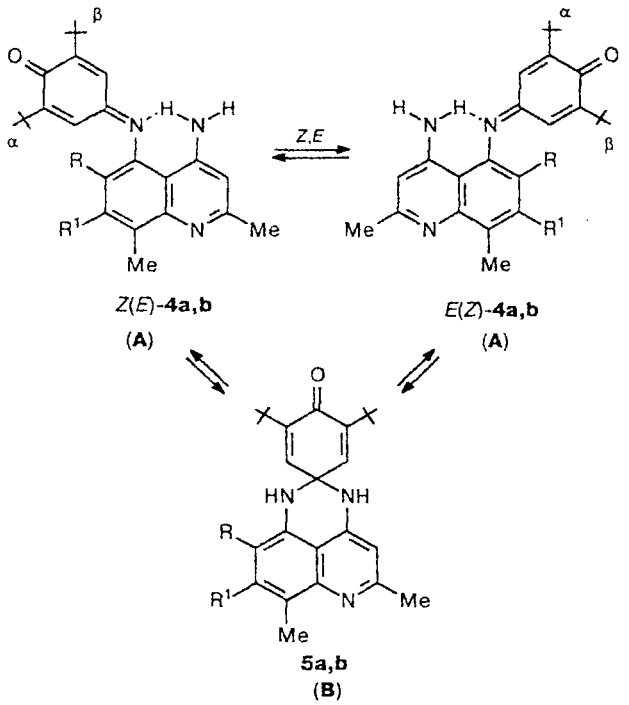

Compounds **4a,b** are violet, whereas compound **5c** is yellow, which is typical of cyclic structures.[3] The IR spectrum of **5c** has two absorption bands of the amino groups (at 3150 and 3353 cm^{-1}). The ^{1}H NMR spectrum indicates that the *tert*-butyl groups are equivalent (1.37, singlet, 18 H).

When dissolved in polar solvents, quinone imines **4a,b** were partially converted to spiranes **5a,b**. After prolonged storage of solutions (from several days to 2—3 weeks) at 20 °C, the **4a,b** (**A**) ⇌ **5a,b** (**B**) equilibrium was established with the spirane form predominating (73% and 61% for **5a** and **5b**, respectively).

When solutions of compounds **4a,b** in $C_6D_5NO_2$ were heated above 100 °C, broadening of two peaks of the *tert*-butyl groups of the quinone imine forms was observed, and the integrated intensity of the 18-proton peak of spirane forms **5a,b** was decreased.

This spectral behavior is associated with the occurrence of the degenerate $Z \rightleftharpoons E$ topoisomerization of quinone imines **4a,b** with respect to the C=N bond, which is accompanied by the reversible structural rearrangement (see Scheme 2). The kinetic, activation, and thermodynamic parameters of the Z,E conversions under consideration and the **4a,b** ⇌ **5a,b** tautomeric equilibrium are summarized in Table 3.

As can be seen from Table 3, the additional methyl group at position 7 of the quinoline ring of molecule **4b** substantially increases (by 1.5 kcal mol^{-1}) the activation barrier of the degenerate Z,E stereoconversions compared to **4a**. However, in the case of the **A** ⇌ **B** ring-chain equilibrium under the standard conditions, the energy gap ($\Delta G_{298}°$) is substantially smaller (by ~0.6 kcal mol^{-1}) for the **4b** ⇌ **5b** conversion than for the **4a** ⇌ **5a** equilibrium.

The fundamental differences in the behavior of these compounds are observed in the dynamics of the change in the shape of the signals of the *tert*-butyl groups as the temperature of solutions changes. Thus, in the case of compounds **4a** and **5a**, synchronous broadening of all the signals of the *tert*-butyl groups occurs, which indicates that the Z,E stereoconversion of quinone imine **4a**

Table 3. Kinetic, activation, and thermodynamic parameters of the Z,E stereodynamics and the **4a,b** ⇌ **5a,b** tautomeric equilibrium

Compound	Process	T/K	k/s^{-1}	$\Delta G_{248}^{\neq}$	$\Delta H^{\neq}$	$\Delta S^{\neq}$	Ratio (%)		ΔG_{248}^{0}	ΔH^{0}	ΔS^{0}
				kcal mol^{-1}		cal (mol K)$^{-1}$	A	B	kcal mol^{-1}		cal (mol K)$^{-1}$
4a	*Z*-**4a** ⇌ *E*-**4a**	393	1.7	22.5	22.5±0.2	0.0±0.5	36.8	63.2	1.54	5.03±0.02	11.73±0.06
	4a$_{(A)}$ ⇌ **5b**$_{(B)}$	423	19.8				51.4	48.6			
4b	*Z*-**4b** ⇌ *E*-**4b**	393	0.36	24.0	24.0±0.1	0.0±0.4	42.2	57.8	0.96	3.47±0.02	8.42±0.05
	4b$_{(A)}$ ⇌ **5b**$_{(B)}$	453	24.0				55.0	45.0			

and its tautomeric rearrangement to spirane **5a** proceed at the same rate. Therefore, the **4a** ⇌ **5a** tautomeric processes and the *Z*-**4a** ⇌ *E*-**4a** stereoconversions are rigidly coupled.

On the contrary, the spectral behavior of compounds **4b** and **5b** indicates that the *Z*-**4b** ⇌ *E*-**4b** and **4b** ⇌ **5b** processes are not synchronized. However, substantial broadening of the signals of the *tert*-butyl groups of quinone imine **4b** is observed at 140—150 °C, which corresponds to the rapid *Z*,*E* interconversion ($k_{Z,E} \geq 24\ s^{-1}$, $T = 180$ °C). The singlet of the *tert*-butyl groups of spirane **5b** is only slightly broadened, which is indicative of the substantially lower rate ($k_{(4b \rightleftharpoons 5b)} \leq 1.2\ s^{-1}$, $T = 180$ °C) of the ring-chain conversion.

The alternative pathways of the *Z* ⇌ *E* stereoconversions of quinone imines **4a,b**, namely the inversion (*i*) and torsion (*t*) pathways, are shown in Scheme 3. Only the torsion pathway may result in spirocyclization due to the polarization of the C=N bond favorable for the *N*,*N*′-proton transfer.

To determine the contribution of the stage of the *N*,*N*′-proton shifts to the kinetics of the **4a,b** ⇌ **5a,b** ring-chain conversion, the labile protons in quinone imine **4a** were replaced by deuterium atoms by double recrystallization of **4a** from deuteromethanol. The temperature dependence of the shape of the line of the *tert*-butyl groups of deuterated imine **4a** is indicative of the absence of a noticeable effect on the kinetics of the

Scheme 3

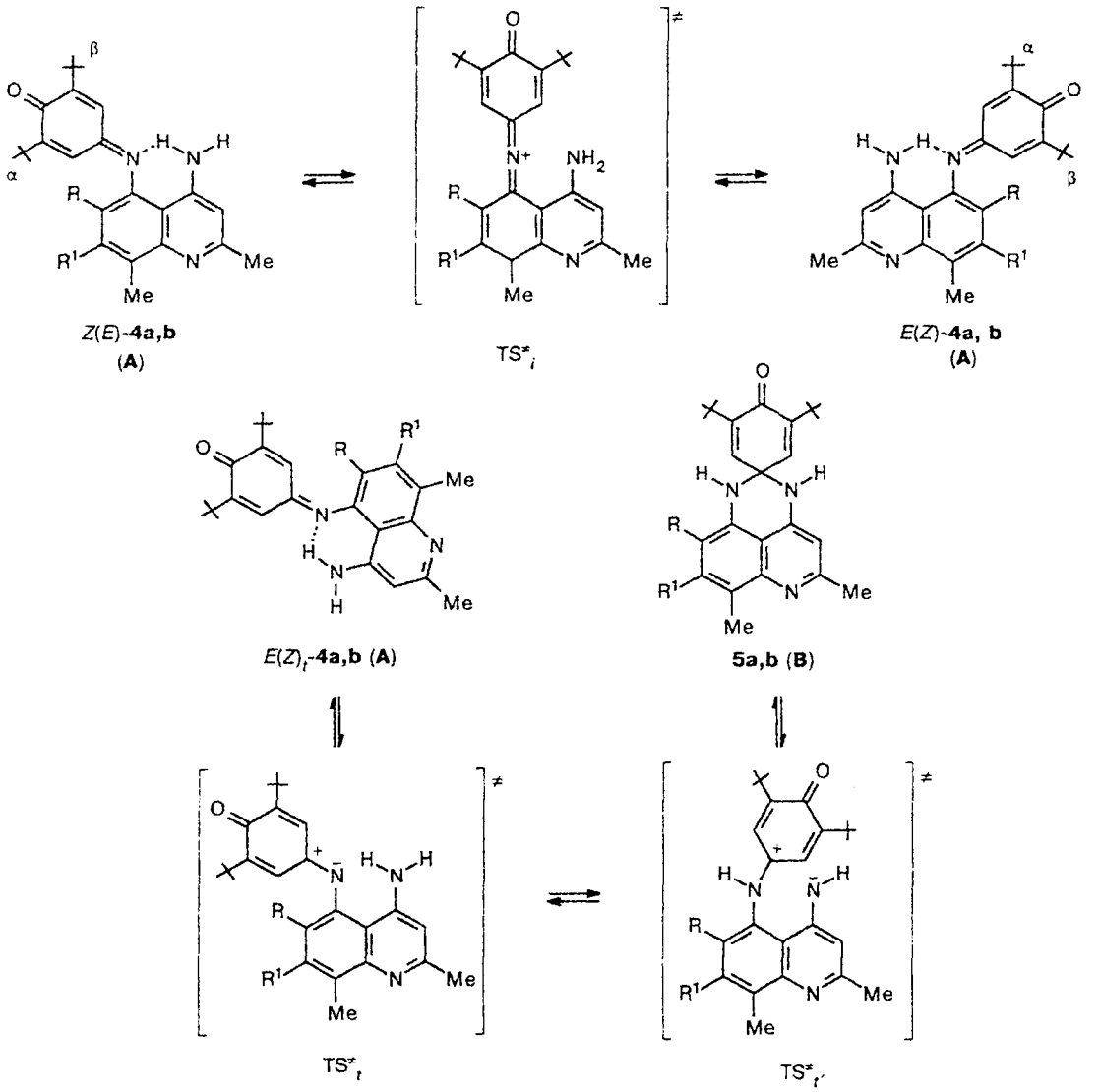

4a ⇄ **5a** rearrangement. Therefore, the *Z,E* stereoconversion, which induces spirocyclization (**4a,b** → $TS_t^{\neq}$), makes the major energy contribution to the activation barrier of this ring-chain rearrangement. In the reverse process, the contribution is determined by the energy that is spent for the cleavage of the C—N bond (**5a,b** → $TS_{t'}^{\neq}$).

Against the background of the absence of the kinetic effects of the replacement of H atoms by D atoms, which are directly involved in the **4a,b** ⇄ **5a,b** reaction, the particularly surprising thing is that the effect of the additional methyl group at position 7 of the quinoline ring of compound **4b**, which is rather remote from the reaction center, is sufficiently large for the *Z*-**4b** ⇄ *E*-**4b** and **4b** ⇄ **5b** processes to become asynchronous. The activation barrier of the latter process is higher than that of the former by almost 3 kcal mol^{-1}. Apparently, this effect is associated with increase in the probability of occurrence of the *Z,E* conversions through the planar inversion (**4a,b** → $TS_t^{\neq}$), which is not productive for the N ⇄ N′ proton transfer and spirocyclization.

Based on the data of UV spectra in nonpolar solvents (benzene, octane, toluene, and chloroform), compounds **4a,b** (Fig. 2, *a*, *b*) occur predominantly in the opened form, whereas compound **4c** (Fig. 2, *c*) occurs in the spirane form. The low intensity absorption band at 550—600 nm is observed in the long-wave region of the spectrum of compound **4c**. The position of this band virtually coincides with those of the bands of the quinone imine structures of compounds **4a,b**.

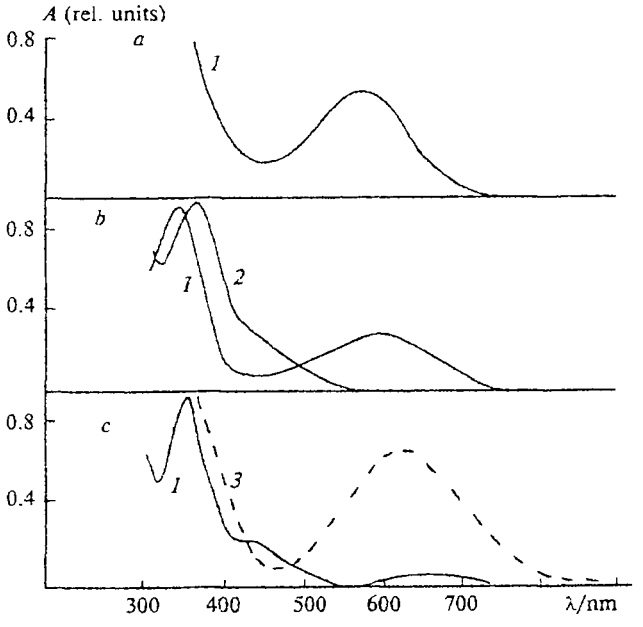

Fig. 2. Absorption spectra of compounds **4a—c** before irradiation (*1*, benzene; and *2*, ethanol) and after irradiation (*3*) (λ_{irrad} = 365 nm, τ_{irrad} = 4200 s): (*a*) **4a**: $2.29 \cdot 10^{-4}$ mol L^{-1}, benzene, d_c = 1.000 cm (d_c is the diameter of the cell); (*b*) **4b**: (*1*) $4.39 \cdot 10^{-5}$ mol L^{-1}, benzene, d_c = 1.000 cm; and (*2*) $5.07 \cdot 10^{-4}$ mol L^{-1}, ethanol, d_c = 0.199 cm; and (c) **4c**: $3.93 \cdot 10^{-4}$ mol L^{-1}, benzene : triethylamine = 115 : 1, d_c = 1.000 cm.

In polar solvents (ethanol and acetonitrile), compounds **4a,b** (immediately after preparation of solutions) exist as quinone imines. The absorption spectra of these compounds are slightly shifted to the short-wave region compared to the spectra obtained in nonpolar solvents. However, after prolonged storage of solutions in the dark (over a period of 100 h), the spectra were changed and became similar to those of compound **4c** in nonpolar solvents. The obtained data indicate that the spirocyclic form is thermodynamically stable for compounds **4a,b** in polar solvents.

Compound **4c** exists in the spirane form in polar solvents (ethanol and acetonitrile) as well. In the electronic spectra, the absorption band in the 550—600 nm region is absent. Irradiation of the spirane form of compounds **4a—c** in nonpolar solvents did not cause its photoconversion to the quinone imine form. Irradiation of solutions of these compounds with light (at 313 and 365 nm) did not result in the appearance of the absorption band typical of the colored form. Unlike spiranes of the perimidine series,[3] the introduction of a nucleophilic agent (morpholine or triethylamine) did not give the desired results.

Photolysis of solutions of compound **4c** in nonpolar solvents (octane and benzene) caused the reversible increase in the low intensity absorption band at 660 nm (Fig. 2, *c*), which indicates that compound **4c** exhibits photochromic properties.

The introduction of a nucleophilic agent (morpholine or triethylamine) makes it possible to substantially slow down the process of dark recovering of the initial absorption spectrum of compound **4c**. Prolonged photolysis (70 min, λ = 365 nm) of these solutions leads to the change in the spectrum, which is characterized by several isobestic points and converts to the final spectrum remaining unchanged after subsequent irradiation. Analogous properties, as in the case of spiranes of the perimidine series,[3] provide evidence that the spirane structure of compound **4c** is completely converted to the quinone imine form after this photolysis, and the intensity of the long-wave absorption band of this structure can be determined from the experimental conditions (benzene, 597 nm, ε = 1700 m^{-1} cm^{-1}).

Experimental

The IR spectra were recorded on a Specord IR-75 instrument as Nujol mulls. The electronic spectra were measured on a Specord M-40 instrument. Photolysis of solutions of the compounds under study were carried out with the use of nonfocused radiation of a DRSh-250 mercury lamp. Individual lines were separated using standard filters in 0.199-cm and 1.000-cm quartz cells.

The ^1H NMR spectra were recorded on a Varian XL-100 spectrometer (100 MHz).

Table 4. Atomic coordinates ($\times10^4$; for H, $\times10^3$) in the structure of **5c**

Atom	x	y	z	Atom	x	y	z	Atom	x	y	z
O(1′)	0966(2)	6323(3)	7532(2)	C(10)	4752(2)	4677(3)	8672(2)	H(13′)	167(2)	588(4)	584(2)
C(1′)	1676(2)	6365(3)	7726(2)	C(11)	6366(2)	5485(4)	7199(2)	H(14′)	214(2)	291(4)	593(2)
C(2′)	2072(2)	7462(3)	8302(2)	C(12)	3764(2)	2829(4)	10180(2)	H(14′)	264(2)	285(4)	684(2)
C(3′)	2832(2)	7318(3)	8610(2)	C(13)	6183(2)	1606(4)	9169(2)	H(14′)	279(2)	412(4)	622(2)
C(4′)	3332(2)	6147(3)	8412(2)	O(1s)	7985(2)	5477(4)	10538(2)	H(2n)	321(2)	494(4)	932(2)
C(5′)	2922(2)	5239(3)	7735(2)	O(2s)	9058(2)	5136(3)	10076(2)	H(3n)	394(2)	741(4)	785(2)
C(6′)	2167(2)	5307(3)	7404(2)	C(1s)	7922(2)	4487(4)	9234(3)	H(3)	517(2)	702(4)	741(2)
C(7′)	1583(2)	8691(3)	8524(2)	C(2s)	8318(2)	5086(4)	9989(2)	H(7)	505(2)	156(4)	1002(2)
C(8′)	2095(2)	9764(4)	9062(2)	C(3s)	9531(2)	5671(5)	10853(2)	H(11a)	639(2)	643(4)	704(2)
C(9′)	975(2)	8130(4)	8977(2)	C(4s)	9623(3)	7174(5)	10807(3)	H(11b)	686(2)	513(4)	743(2)
C(10′)	1169(2)	9454(4)	7768(2)	H(3′)	309(2)	796(4)	898(2)	H(11c)	617(2)	515(4)	668(2)
C(11′)	1769(2)	4308(3)	6733(2)	H(5′)	325(2)	463(4)	754(2)	H(12a)	325(2)	256(4)	988(2)
C(12′)	1239(2)	3278(4)	7056(2)	H(3′a)	253(2)	1015(4)	881(2)	H(12b)	371(2)	369(4)	1055(2)
C(13′)	1293(2)	5148(3)	6030(2)	H(8′b)	176(2)	1052(4)	920(2)	H(12c)	395(2)	193(4)	1055(2)
C(14′)	2376(2)	3466(4)	6398(2)	H(8′c)	237(2)	933(4)	957(2)	H(13a)	617(2)	85(4)	955(2)
N(1)	5926(1)	4071(3)	8186(1)	H(9′a)	58(2)	744(4)	864(2)	H(13b)	669(2)	212(4)	932(2)
N(2)	3590(1)	5304(3)	9139(1)	H(9′b)	65(2)	887(4)	910(2)	H(13c)	620(2)	124(4)	864(2)
N(3)	4030(1)	6776(3)	8205(1)	H(9′c)	121(2)	770(4)	947(2)	H(1sa)	809(3)	375(6)	892(3)
C(2)	5816(2)	5232(4)	7747(2)	H(10′)	88(2)	1017(4)	788(2)	H(1sb)	751(3)	448(6)	920(3)
C(3)	5210(2)	6195(3)	7747(2)	H(10′)	78(2)	880(4)	741(2)	H(1sc)	804(3)	500(6)	876(3)
C(4)	4657(2)	5906(3)	8192(2)	H(10′)	154(2)	993(4)	756(2)	H(3sa)	927(3)	537(6)	1134(3)
C(5)	4207(2)	4354(3)	9153(2)	H(12′)	154(2)	278(4)	748(2)	H(3sb)	1018(3)	507(6)	1089(3)
C(6)	4321(2)	3189(4)	9649(2)	H(12′)	100(2)	266(4)	662(2)	H(4sa)	906(3)	765(6)	1072(3)
C(7)	4982(2)	2335(3)	9641(2)	H(12′)	85(2)	375(4)	722(2)	H(4sb)	978(3)	744(6)	1033(3)
C(8)	5510(2)	2585(3)	9166(2)	H(13′)	107(2)	453(4)	558(2)	H(4sc)	993(3)	761(6)	1137(3)
C(9)	5404(2)	3801(3)	8671(2)	H(13′)	90(2)	574(4)	618(2)				

4-Chloro-5-nitroquinolines, which were used as starting compounds in the synthesis of 5-amino-4-chloroquinolines, were prepared according to a procedure reported previously.[1]

4-Chloro-2,7,8-trimethyl-5-nitroquinoline, cream-colored crystals, yield 97%, m.p. 117—118 °C (from 2-propanol). IR, ν/cm^{-1}: 1460, 1514 (NO_2). Found (%): C, 57.26; H, 4.55; Cl, 14.24; N, 11.19. $C_{12}H_{11}ClN_2O_2$. Calculated (%): C, 57.50; H, 4.42; Cl, 14.14; N, 11.17.

4-Chloro-2,6,8-trimethyl-5-nitroquinoline, pale yellow crystals, yield 98.13%, m.p. 100—101 °C (from 2-propanol). IR, ν/cm^{-1}: 1460, 1527 (NO_2). Found (%): C, 57.83; H, 4.98; Cl, 14.90; N, 11.23. $C_{12}H_{11}ClN_2O_2$. Calculated (%): C, 57.50; H, 4.42; Cl, 14.14; N, 11.17.

Preparation of 5-amino-4-chloroquinolines (1b,c) (general procedure). A mixture of 4-chloro-5-nitroquinoline (0.148 mol), powdered Fe (60 g), H_2O (100 mL) acidified with 1—2 drops of glacial AcOH, and *o*-xylene (100 mL) was boiled with vigorous stirring for 6 h. A solution of NaOH (2 g) in H_2O (20 mL) was added. The reaction mixture was boiled with stirring for 10—15 min and cooled. The residue was filtered off. The organic layer was separated. The iron residue was treated with boiling chloroform (3×25 mL). The chloroform and *o*-xylene solutions were combined. Distillation of the solvents gave 5-amino-4-chloroquinolines (**1b,c**).

5-Amino-4-chloro-2,7,8-trimethylquinoline (1b), yellow crystals, yield 82.5%, m.p. 129—130 °C (from heptane). IR, ν/cm^{-1}: 3346, 3486 (NH_2). Found (%): C, 65.34; H, 6.00; Cl, 16.00; N, 12.75. $C_{12}H_{13}ClN_2$. Calculated (%): C, 65.31; H, 5.94; Cl, 16.03; N, 12.69.

5-Amino-4-chloro-2,6,8-trimethylquinoline (1c), bright yellow crystals, yield 80%, m.p. 131—132 °C (from heptane). IR, ν/cm^{-1}: 3396, 3486 (NH_2). Found (%): C, 65.43; H, 5.89; Cl, 16.07; N, 12.80. $C_{12}H_{13}ClN_2$. Calculated (%): C, 65.31; H, 5.94; Cl, 16.03; N, 12.69.

5-Amino-4-(3,5-di-*tert*-butyl-4-hydroxyphenylamino)-2,6,8-trimethylquinoline hydrochloride (3c · HCl). A solution of 5-amino-4-chloro-2,6,8-trimethylquinoline (**1c**) (1.8 mmol) and 4-amino-2,6-di-*tert*-butylphenol (**2**) (3.6 mol) in *o*-xylene (5 mL) was boiled for 3 h. Then the reaction mixture was cooled. The precipitate that formed was filtered off, washed with hexane, and dried. Yellow crystals were obtained in a yield of 0.2 g (25%), m.p. 253—255 °C (from methanol). IR, ν/cm^{-1}: 3500 (OH), 3087, 3166 (NH); 1634, 1600 (arom). Found (%): C, 70.00; H, 8.89; Cl, 8.10; N, 9.46. $C_{26}H_{36}ClN_3O$. Calculated (%): C, 70.64; H, 8.21; Cl, 8.02; N, 9.50.

General procedure for the preparation of spiroquinazolines (5a—c). A solution of 5-amino-4-chloroquinoline (1 mmol) and 4-amino-2,6-di-*tert*-butylphenol (**2**) (1.6 mmol) in *o*-xylene (5 mL) was boiled for 3 h. The reaction mixture was cooled. A 25% aqueous ammonia solution (1 mL) and $CHCl_3$ (5—7 mL) were added. The reaction mixture was kept for 1 day. Then the solution was passed through a column packed with Al_2O_3 (l = 30 cm, d = 1.5 cm, a 1 : 5 AcOEt—hexane mixture was used as the eluent). The violet fraction was collected. After evaporation of the solvent, products **5a—c** were obtained.

2′,6′-Di-*tert*-butyl-5,7-dimethylspiro[6-aza-2,3-dihydroperimidine-2,4′-cyclohexa-2′,5′-dien]-1′-one (5a), yield 94.6%, violet crystals, which turn yellow at 135—145 °C and melt at 213—215 °C (from acetonitrile). IR, ν/cm^{-1}: 3165, 3326, 3452 (NH), 1634, 1648 (C=O). Found (%): C, 77.11; H, 7.96; N, 10.60. $C_{25}H_{31}N_3O$. Calculated (%): C, 77.08; H, 8.02; N, 10.78. ^1H NMR ($C_6D_5NO_2$), δ 1.34 (s, 4 H, Bu^t); 1.38 (s, 6 H, Bu^t); 1.48 (s, 8 H, Bu^t); 2.7 (s, 2 H, CH_3); 2.74 (s, 1 H, CH_3); 2.83 (s, 1 H, CH_3); 2.86 (s, 2 H, CH_3); 5.50 (s, 1 H, NH); 6.00 (s, 1 H, NH). UV (benzene), λ/nm (ε): 551.9 (4360).

2′,6′-Di-*tert*-butyl-5,7,8-trimethylspiro[6-aza-2,3-dihydroperimidine-2,4′-cyclohexa-2′,5′-dien]-1′-one (5b), yield 68.3%, violet crystals, which turn yellow at 190 °C and melt at 243—245 °C (from acetonitrile, freezing to −15 °C). IR, ν/cm^{-1}: 3300, 3460 (NH), 1634, 1659 (C=O). Found (%): C, 77.02; H, 7.90; N, 10.20. $C_{26}H_{33}N_3O$. Calculated (%): C, 77.42; H, 8.19; N, 10.42. ^{1}H NMR ($C_6D_5NO_2$) δ: 1.35 (s, 12 H, Bu^t); 1.50 (s, 6 H, Bu^t); 2.60 (s, 3 H, CH_3); 2.71 (s, 3 H, CH_3); 2.80 (s, 3 H, CH_3); 5.35 (s, 1 H, NH); 5.95 (s, 1 H, NH). UV (benzene), λ/nm (ε): 315.5 (19400), 560.5 (6680).

2′,6′-Di-*tert*-butyl-5,7,9-trimethylspiro[6-aza-2,3-dihydroperimidine-2,4′-cyclohexa-2′,5′-dien]-1′-one (5c), yellow crystals, yield 75%, m.p. 240—242 °C (from acetonitrile, freezing to −15 °C). IR, ν/cm^{-1}: 3140, 3226, 3353 (NH), 1640, 1650 (C=O). Found (%): C, 77.21; H, 8.05; N, 10.19. $C_{26}H_{33}N_3O$. Calculated (%): C, 77.42; H, 8.19; N, 10.42. ^{1}H NMR ($C_6D_5NO_2$) δ: 1.37 (s, 18 H, Bu^t); 2.40 (s, 3 H, CH_3); 2.79 (s, 3 H, CH_3); 2.85 (s, 3 H, CH_3), 5.21 (s, 1 H, NH); 6.15 (s, 1 H, NH). UV (ethanol), λ/nm (ε): 322.6 (104500), 400.0 (4200, shoulder).

Crystals of **5c** ($C_{26}H_{42}N_3O \cdot C_4H_8O_2$) are monoclinic, space group $P2_1/c$, at −120 °C: a = 17.556(4), b = 9.473(3), c = 17.079(5) Å, β = 101.92(1)°, V = 2779.1(8) Å, M = 500.73, Z = 4, d_{calc} = 1.197 g cm^{-3}, μ(λMo-Kα) = 0.08 mm^{-1}. The unit cell parameters and intensities of 6690 independent reflections were measured on an automated four-circle Siemens P3/PC diffractometer (λMo-Kα radiation, graphite monochromator, θ/2θ scanning technique, $2\theta_{max}$ = 52°). The structure was solved by the direct method and refined by the full-matrix least-squares method with anisotropic thermal parameters for nonhydrogen atoms. The solvate ethyl acetate molecule was revealed from the difference Fourier map. The positions of the hydrogen atoms were located from the difference Fourier map and refined isotropically with the fixed thermal parameters (U_{iso} = 0.04 Å^2; for the hydrogen atoms of the solvate ethyl acetate molecule, U_{iso} = 0.08 Å^2). The final values of the R factors were as follows: R = 0.053 and R_w = 0.055 using 2792 reflections with $I > 3\sigma(I)$. All calculations were carried out on an IBM PC/AT-386 computer using the SHELXTL PLUS program package (PC Version).[5] The atomic coordinates are given in Table 4.

References

1. V. N. Komissarov, E. N. Gruzdeva, V. A. Kharlanov, V. A. Kogan, and V. I. Minkin, *Zh. Org. Khim.*, 1993, **29**, 2030 [*Russ. J. Org. Chem.*, 1993, **29** (Engl. Transl.)].
2. E. G. Rozantsev and V. D. Sholle, *Organicheskaya khimiya svobodnykh radikalov* [*Organic Chemistry of Free Radicals*], Khimiya, Moscow, 1979, p. 131 (in Russian).
3. V. A. Kharlanov, M. I. Knyazhinskii, and V. E. Kuznetsov, *Zh. Org. Khim.*, 1992, **28**, 1093 [*Russ. J. Org. Chem.*, 1992, **28** (Engl. Transl.)].
4. F. H. Allen, O. Kennard, D. G. Watson, L. Brammer, A. G. Orpen, and R. Taylor, *J. Chem. Soc., Perkin Trans. 2*, 1987, 51.
5. W. Robinson and G. M. Sheldrick, SHELX, in *Crystallographic Computing — Techniques and New Technologies*, Eds. N. W. Isaacs, M. R. Taylor, Oxford, England, Oxford Univ. Press, 1988, 366.

Received March 21, 1997